Calcium-Dependent Conformational Change and Thermal Stability of the Isolated PsbO Protein Detected by FTIR Spectroscopy

P. Heredia and J. De Las Rivas*

Instituto de Recursos Naturales y Agrobiología (CSIC), P.O. Box 257, 37071 Salamanca, Spain

Received April 11, 2003; Revised Manuscript Received July 9, 2003

ABSTRACT: The structure and function of the photosystem II PsbO extrinsic protein is under intense research, being an essential part of the biomolecular engine that carries out water oxidation and oxygen production. This paper presents a structural analysis of the isolated PsbO protein by FTIR spectroscopy, reporting detailed secondary structure quantification and changes in the secondary structure content of the protein attributed to the effect of calcium (Ca^{2+}). Measurements in H_2O and D_2O have allowed us to see the effect of calcium on the conformation of the protein. The results indicate that (i) the protein presents a major content of β-structure (i.e., β-sheet, β-strands, β-turns) as detected by the infrared bands at 1624−1625, 1678−1679, 1688−1689 cm^{-1}, which account for about 38% in water and 33% in heavy water, in the presence of calcium; and (ii) the amount of this β-structure fraction increases 7−10% in the absence of calcium, with a concomitant decrease in loops and nonordered structure. The thermal denaturation profile of the protein in the presence of calcium showed low stability with T_m ∼56 °C. This profile also shows a second phase of denaturation above 60 °C and the appearance of aggregation signals above 70 °C. Our observations indicate that calcium is able to modify the conformation of the protein at least in solution and confirm that PsbO is mainly a β-protein where β-sheet is the major ordered secondary structure element of the protein core.

The reactions resulting in oxygen evolution take place within photosystem II (PSII),[1] a thylakoid membrane inserted multisubunit complex consisting of both intrinsic and extrinsic polypeptides. Photosystem II is present in all known oxyphotosynthetic organisms: cyanobacteria, algae, and higher plants. The structure of this protein complex has been solved by X-ray crystallography in two thermophilic cyanobacteria: *Synechococcus elengatus* at 3.8−4.2 Å resolution (*1*) and *Thermosynechococcus vulcanus* at 3.7 Å resolution (*2*). The main intrinsic proteins of PSII are D1, D2, CP47, CP43, and cytochrome b_{559}, which form the reaction center of this complex. Deletion or inactivation of the genes encoding these key reaction center proteins leads to a complete loss of oxygen evolution. Other smaller proteins are associated with the reaction center; some of them are also inserted in the thylakoid membrane neighboring those high molecular mass polypeptides, and in many cases we still do not know their function (*3*). Other PSII protein subunits are extrinsic and associated to the lumenal side of the complex. It is well documented that, in green algae and higher plants, at least three lumenal extrinsic polypeptides are required to achieve normal and stable oxygen evolution rates. They are encoded in the nuclear genome by the *psbO*, *psbP*, and *psbQ* genes, and all contain a transit peptide that courses them to the thylakoid lumen (*4*). Their apparent molecular masses determined by SDS−PAGE electrophoresis are 33 kDa for PsbO, 23 kDa for PsbP, and 17 kDa for PsbQ. Depletion of these polypeptides impairs normal oxygen evolution, and after this, PSII activity only can be partly recovered by using high concentrations of calcium and chloride (see ref *4* for a review). It should be noted that, in cyanobacteria, PsbP and PsbQ are not present, and the PsbO extrinsic protein is as far as we know accompanied by a 12 kDa protein (PsbU) and a cytochrome c_{550} (PsbV), which are likely to replace the 23 and 17 kDa protein function (*5*−*8*).

Of the extrinsic lumenal proteins, the PsbO protein seems to be the most important for oxygen evolution as its removal severely decreases PSII activity: more than 60% according to ref *9* or even 100% according to ref *10*. It is now known to be one of the closest proteins to the manganese cluster where water oxidation occurs. Given its effect on stabilizing the manganese cluster and because two manganese atoms from the cluster are released into solution in its absence at low chloride levels (*11*), PsbO has been termed the "manganese stabilizing protein" (MSP), although none of the amino acids of this protein are likely ligands to any of the manganese atoms of the cluster (*12*). Complete removal of the PsbO protein from PSII has been achieved using high concentrations of calcium, as well as NaCl−urea or alkaline pH treatment (*10*, *11*, *13*, *14*). After this removal, PsbO behaves as a water-soluble protein, and usually it keeps its ability to rebind to PSII (*10*, *15*). Several studies have focused on determining the activity of PSII, mainly measured as oxygen evolution, in release−reconstitution experiments with PsbO (*10*, *16*, *17*). Site-directed mutagenesis has been used to map the residues involved in the binding of PsbO to PSII (*18*−*21*).

* Corresponding author. Phone: 34-923-219606. Fax: 34-923-219609. E-mail: jrivas@usal.es.

[1] Abbreviations: ANS, 8-anilino-1-naphthalenesulfonate; CD, circular dichroism; EGTA, ethylene glycol bis(β-aminoethyl ether)-*N*,*N*,*N*′,*N*′-tetraacetic acid; FTIR, Fourier transform infrared spectroscopy; PSII, photosystem II.

10.1021/bi034582j CCC: $25.00
Published on Web 09/20/2003

Structural predictions (*22*−*24*) together with structural analyses by low-resolution techniques such as UV CD (*20*, *21*, *25*, *26*), FTIR (*20*, *27*, *28*), tryptophan fluorescence emission (*26*, *29*), or analytical centrifugation (*30*) have provided information about the secondary structure and general shape of this extrinsic polypeptide. Some FTIR and far-UV CD studies (*20*) supported the idea of a "natively unfolded" conformation in solution due to its high amount of random coil (or nonordered) structure and other features common to known natively unfolded proteins. Different studies proposed a "molten globule" conformation (*31*) with a hydrophobic β-sheet core (*26*, *29*). This idea was later supported by a 3D threading model that proposed a majority β-structure probably folded as two domains (*24*). The structural data obtained more recently from the crystals of cyanobacterial PSII (*1*, *2*) confirm that PsbO within PSII is mainly a β-protein probably folded as a kind of β-barrel. The structural information about PsbO contained in these PSII crystals, PDB 1FE1 (*1*) and PDB 1IZL (*2*), is still partial since the resolution on this subunit is lower than average and only a fraction of the PsbO carbon skeleton has been assigned to the structure. In addition, the specific PsbO residues (i.e., lateral chains) are not given. Therefore, the detailed atomic structure of PsbO remains unsolved. Some authors have obtained some small dimer crystals of isolated PsbO, but they do not diffract well enough to be resolved (*32*).

It is well established that PsbO can be removed from PSII using high calcium concentrations. The identification of this metal as an important cofactor for oxygen evolution has increased the interest in determining the role of calcium in PSII (reviewed in ref *33*) and its relation with PsbO (*34*−*36*). Research has been done about the binding affinity and the location of the binding sites for this metal in PSII (*34*−*37*). PsbO isotope editing and FTIR studies of its rebinding to PSII reaction centers have reported that the β-sheet structure content of PsbO increases upon binding to PSII (*38*). Following the ideas about conformational changes of this protein and the role of calcium, in this paper we focus on the possible action of calcium upon the structure of isolated PsbO as measured by FTIR spectroscopy. The results have led us to conclude that the presence or absence of calcium, respectively, decreases or increases the amount of β-sheet secondary structure of the PsbO extrinsic protein, and this change may be an important step in the way this protein is able to bind to PSII and stabilize the function of the oxygen evolving complex.

MATERIALS AND METHODS

Protein Purification. PSII-enriched membranes were isolated from market spinach (*Spinacia oleracea*) as described in ref *39* with some minor modifications (*40*). PSII activity of the isolated membranes was measured with a Clark-type oxygen electrode at 20 °C and showed an activity of about 600−650 μmol of O_2/(mg of chlorophyll·h) in a 50 mM MES−NaOH, pH 6.0, 0.33 M sorbitol, 5 mM NaCl, 5 mM $CaCl_2$, and 2 mM $NaHCO_3$ buffer, supplemented with 250 μM 2,6-dichloro-*p*-benzoquinone (DCBQ) and 3.5 mM $K_3Fe(CN)_6$. All protein purification steps were performed on ice or at 4 °C. The PsbO extrinsic protein was extracted from PSII-enriched membranes by a first treatment with a solution containing 50 mM Mes−NaOH, pH 6.0, and 1 M NaCl, to remove PsbP and PsbQ extrinsic proteins, for 1 h at a chlorophyll concentration of 0.5 mg/mL. PSII-enriched membranes containing the PsbO extrinsic protein were recovered by centrifugation at 48000*g* for 20 min. The supernatant was discarded, and the pellet was resuspended again in the former medium and centrifuged again. The pellet was resuspended in a second medium containing 50 mM Mes−NaOH, pH 6.0, and 1 M $CaCl_2$ to remove PsbO extrinsic protein and centrifuged again. The supernatant was recovered, desalted (until $[Ca^{2+}]_{final} \leq 0.125$ mM), and concentrated using VIVASPIN-20 and/or VIVASPIN-2 tubes (Sartorius). The concentrate was centrifuged at 48000*g* to remove a pale green precipitate and loaded onto a DEAE-Sepharose column equilibrated with several volumes of 50 mM Mes−NaOH, pH 6.0. PsbO protein was eluted with a 0−0.7 M NaCl gradient with the protein eluting at about 150 mM NaCl. Fractions containing the pure protein were pooled and concentrated. Protein purity was tested by SDS−PAGE (*41*), and the degree of purity was always above 97%. Protein concentration was determined by the bicinchoninic acid (BCA) method (Pierce).

FTIR Sample Treatment and Spectrum Recording. Concentrated PsbO extrinsic protein was exchanged using VIVASPIN-2 tubes (Sartorius) to a buffer containing 50 mM Mes−NaOH, pH 6.0, 0.33 M sorbitol, 5 mM NaCl, and 1 mM $CaCl_2$ (buffer A) or in this buffer where 1 mM $CaCl_2$ was replaced by 1 mM ethylene glycol bis(β-aminoethyl ether)-*N*,*N*,*N*′,*N*′-tetraacetic acid (EGTA) (buffer B), depending on the experiment. To obtain total exchange, 150 μL of the protein sample at about 20 mg/mL was washed three times with 1 mL of buffer A or buffer B. For samples in D_2O the buffer used was 50 mM Mes−NaOD, pD 6.0, keeping the rest the same. The protein concentration used for H_2O experiments was always between 30 and 35 mg/mL while for D_2O experiments it was 25−30 mg/mL. The experiments were done always with freshly isolated protein. For infrared spectroscopy analyses a Nicolet Nexus 670 FTIR spectrometer equipped with a MCT/A detector and a Ge−KBr beam splitter was used. Samples were located in a liquid cell between two 32 × 3 mm CaF_2 windows (Wilmad Glass Co. Inc.) with a path length spacer of 6 μm (Harrick Scientific Co.). For each measurement, a volume of 30 μL of sample was used to fill the cell. For each spectrum 1000 interferograms were averaged, apodized with a Happ-Genzel function, no zero filling, and Fourier transformed to give a nominal resolution better than 2 cm^{-1}. Other measurement conditions were as follows: scan speed 2.53 cm s^{-1}, wavenumber range 4000−650 cm^{-1}, and temperature 20 °C. Background correction was obtained by measuring the background before each sample and automatic subtraction. The sample chamber was closed and connected to a CD7 air-dryer (Atlas Copco) that provided air with very low water vapor level (ice point lower than −70 °C). The buffer signal in each sample was removed by subtraction of the infrared spectra of the corresponding buffer from the spectra of each sample. We repeated several times the FTIR measurements, and we did that using aliquots of the same preparation and preparations that showed a uniform stable amide I line shape. For heat treatment, a recirculating bath was used, and the temperature was controlled around the cell with a thermocouple.

Spectrum Processing and Analyzing. Subtraction curves were obtained with OMNIC sofware, using deconvolution

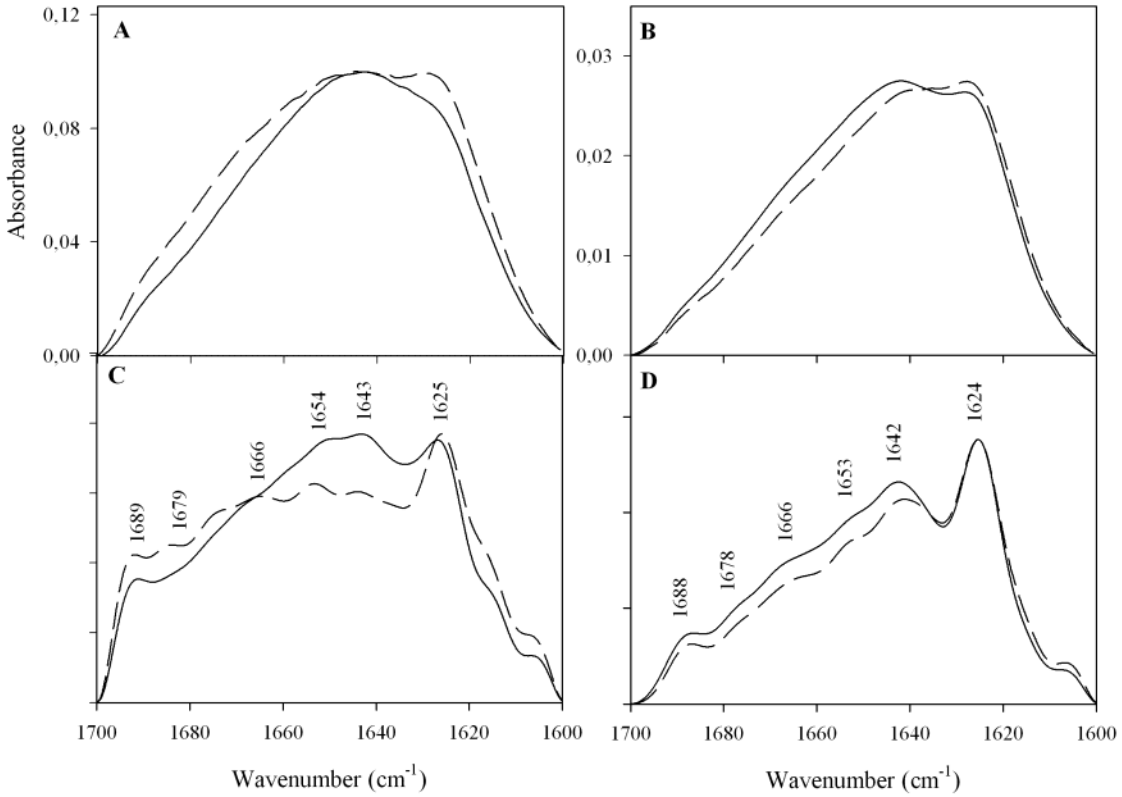

FIGURE 1: Amide I band in H_2O (A) and amide I′ band in D_2O (B) spectra of the PsbO protein with the addition of 1 mM $CaCl_2$ (solid line) or 1 mM EGTA (dashed line). Panels C and D show the deconvolution of the spectra of panels A and B, respectively.

with parameters $k = 2$ and half-width = 18. Second derivatives were obtained with RAMOPN software. Curve fitting to a mixture between Lorentzian and Gaussian curves was done with SPECTRACALC software following the criteria indicated in ref *42*. The quality of the fitting was good given that χ^2 values were always below 10^{-5}. Quantification of the amide band components was calculated for at least three independent measurements, and average and standard deviation for each component are given.

RESULTS

The isolation and purification of the native PsbO protein following the protocol described in Materials and Methods were successful, achieving a purity above 97% (as detected by SDS−PAGE). All of the FTIR measurements were done with freshly isolated protein, and in these conditions samples were uniform in their amide band line shape. The samples used for experiments in the presence of calcium or EGTA were aliquots of the same preparation.

FTIR spectra between 1700 and 1600 cm^{-1} of isolated PsbO are presented in Figure 1. The panels show the PsbO protein spectra of the amide I band in H_2O (A) and the amide I′ band in D_2O (B) with $CaCl_2$ (solid line) and with EGTA (dashed line). The amide band with calcium, both in H_2O and in D_2O (Figure 1A,B, solid lines), is centered around 1640 cm^{-1} and presents a shoulder around 1625 cm^{-1} that is more prominent in D_2O. These signals are better observed in the deconvoluted spectra (Figure 1C,D). The deconvolution allows identification of the position of six main bands in the infrared spectra of PsbO. These bands are 1625−1624, 1643−1642, 1654−1653, 1666, 1679−1678, and 1689−1688 cm^{-1}. The number and positions of the bands are similar both in H_2O and in D_2O, with a small isotopic displacement of 1 cm^{-1} for the samples in D_2O. The spectra with EGTA (Figure 1A,B, dashed lines) show a clear increase of the band at 1625−1624 cm^{-1}, which in the case of D_2O overtakes the central peak, indicating an apparent change in relative proportions. These qualitative observations were verified when the decomposition and quantification of each band on the spectra were obtained (Figure 3 and Table 1).

Figure 2A shows the infrared deconvoluted spectra between 1800 and 1600 cm^{-1} of a PsbO protein sample in D_2O, which had not been fully $CaCl_2$ depleted. The $CaCl_2$ concentration in both samples was around 5 mM. The solid line represents this non-$CaCl_2$-depleted protein sample plus 1 mM $CaCl_2$, and the dashed line reflects this protein sample plus the addition of 1 mM EGTA. The latter is not enough to fully chelate the remaining $CaCl_2$ concentration. No significant difference between the $CaCl_2$- and the EGTA-treated samples can be seen. The plot is a control to demonstrate that the amplitude increment of the 1625−1624 cm^{-1} band shown in Figure 1B with the addition of EGTA is a protein structural change that cannot be assigned to the EGTA presence in this buffer, i.e., to the direct effect of this chelator upon the protein, but it is rather due to the depletion of calcium. We tried to check the reversibility of the effect. When $CaCl_2$ was added back in sufficient amount (5−10 mM $CaCl_2$) to samples previously treated with EGTA (i.e., samples which will be expected to give a spectrum similar to that in Figure 1A, dashed line) the change mostly disappeared (data not shown). This feature suggests that the effect is reversible, but these measurements were indirect because they had to be done with different aliquots, since a

Table 1: Quantification of the Different Components Present in the Amide I and Amide I′ FTIR Bands of the PsbO Extrinsic Protein with $CaCl_2$ and EGTA[a]

% area of amide I (H_2O)			% area of amide I′ (D_2O)			
position	+$CaCl_2$	+EGTA	position	+$CaCl_2$	+EGTA	assignment
1689	1.69 ± 0.46	1.32 ± 0.09	1688	2.13 ± 0.25	1.81 ± 0.22	β-sheet
1679	9.07 ± 1.37	15.64 ± 1.11	1678	2.47 ± 1.19	2.51 ± 1.51	turns, β-sheet
1666	15.48 ± 0.48	9.25 ± 1.75	1666	24.04 ± 0.44	21.21 ± 0.91	turns, loops
1654	21.33 ± 2.87	21.61 ± 1.54	1653	11.10 ± 1.49	12.30 ± 1.36	α-helix
1643	23.02 ± 1.59	19.63 ± 2.16	1642	30.53 ± 2.17	25.33 ± 1.56	nonordered
1625	27.98 ± 1.84	31.54 ± 0.16	1624	28.65 ± 0.80	35.19 ± 0.97	β-sheet

[a]Data correspond to the average and standard deviations of three different experiments.

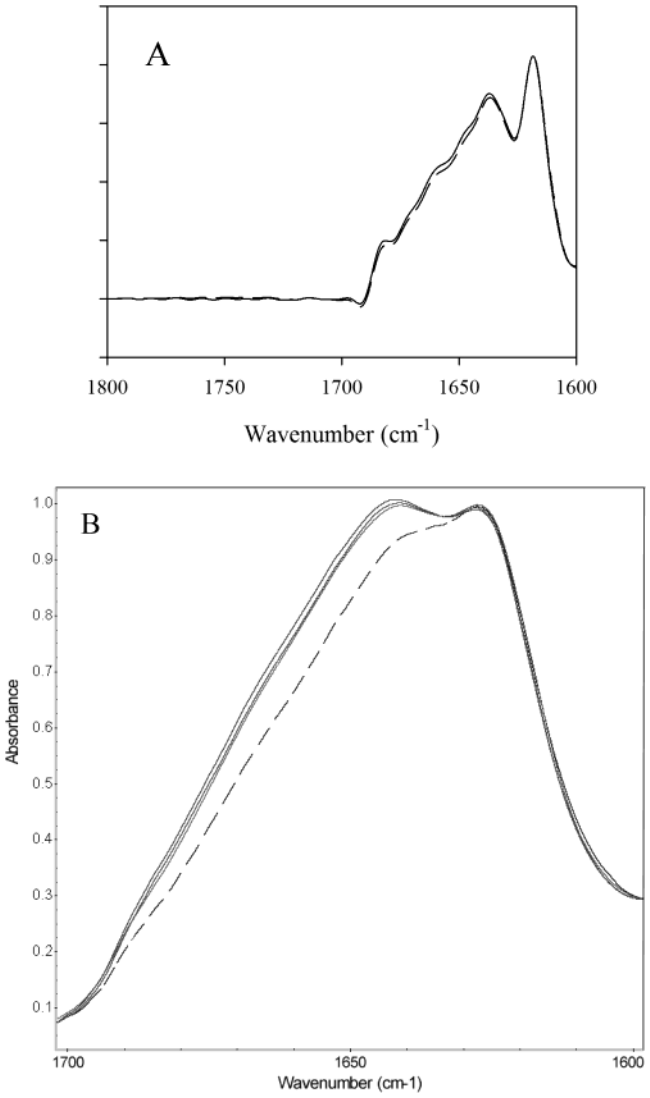

FIGURE 2: (A) FTIR deconvoluted spectra of PsbO not fully $CaCl_2$ depleted (aproximately 5 mM $CaCl_2$) plus 1 mM $CaCl_2$ (solid line) and plus 1 mM EGTA (dashed line). (B) FTIR spectra of the PsbO amide I′ band in D_2O with different concentrations of $CaCl_2$ [0.5, 1, and 5 mM (consecutive solid lines)] or with 1 mM EGTA (dashed line).

sample once introduced in the FTIR cell cannot be recovered.

Another important control to check the specificity of the effect of calcium upon PsbO was to use several calcium concentrations. Figure 2B shows the spectra of the amide I′ band of PsbO with no calcium (dashed line) and with three different increasing calcium concentrations of 0.5, 1, and 5 mM. The calcium concentrations of the spectra correspond to a stimated calcium/protein ratio of about 1, 2, and 10, respectively. The calculation of these ratios is not easy because the protein concentration used in the FTIR measurements, as indicated in Materials and Methods, has to be very high. Despite these practical considerations the results in Figure 2B show a clear difference between the calcium-depleted sample and the samples with calcium. The effect of the addition of calcium seems to be quite cooperative and rather saturated. To quantify these effects, we calculated the area of the amide I′ band for each calcium concentration. To do this, the spectra were normalized to the band at 1624 cm^{-1} and to both extremes of the amide band (i.e., 1700 and 1600 cm^{-1}) (see Figure 2B). The area integrations were done correcting also the baseline between limits 1700 and 1600 cm^{-1}. The data obtained gave an area ratio of 1.11, 1.13, and 1.15 for the consecutive spectra with 0.5, 1, and 5 mM calcium, all taking as reference the calcium-depleted sample (i.e., area value 1.00). These numbers indicate that with about 1 calcium per protein we see an 11% global change; and that about 10 times more calcium only produces a 4% additional increase in the FTIR-detected conformational change. Therefore, the concentration used in the rest of the measurements (1 mM calcium) is very close to saturation. Finally, as another control in a different experiment we use buffers that have the same composition as buffers A and B (described in Materials and Methods) but with 5 mM $MgCl_2$ present. The presence of this salt with magnesium in our observations does not seem to affect the IR spectra. The spectra of samples with EGTA (calcium-depleted samples) and with EGTA plus $MgCl_2$ were similar to the spectra in the dashed line of Figure 2B.

Figure 3 presents the results of the decomposition and fitting of the infrared spectra from isolated PsbO in H_2O (panels A and B) and in D_2O (panels C and D) and in the presence of 1 mM $CaCl_2$ (panels A and C) or EGTA (panels B and D). The quantification of the bands that form each spectrum is presented in Table 1. This decomposition and quantification reflect in numbers the effects observed in the amide band of PsbO when calcium depletion occurs. For the samples in H_2O, the numbers show an increase in the 1625 cm^{-1} band of about 4% and a concomitant decrease of the 1643 cm^{-1} band of about 4%. At the same time, there is a 6% decrease of the 1666 cm^{-1} band and a similar increase in the 1679 cm^{-1} band. These data indicate approximately a 10% change in structure when PsbO samples are calcium depleted. For the samples in D_2O, the numbers show an increase in the 1624 cm^{-1} band of around 7% that can be correlated with a decrease of the 1643 cm^{-1} band of about 5% plus a decrease of about 3% in the 1666 cm^{-1} band. These data indicate a change in structure of 7−8%.

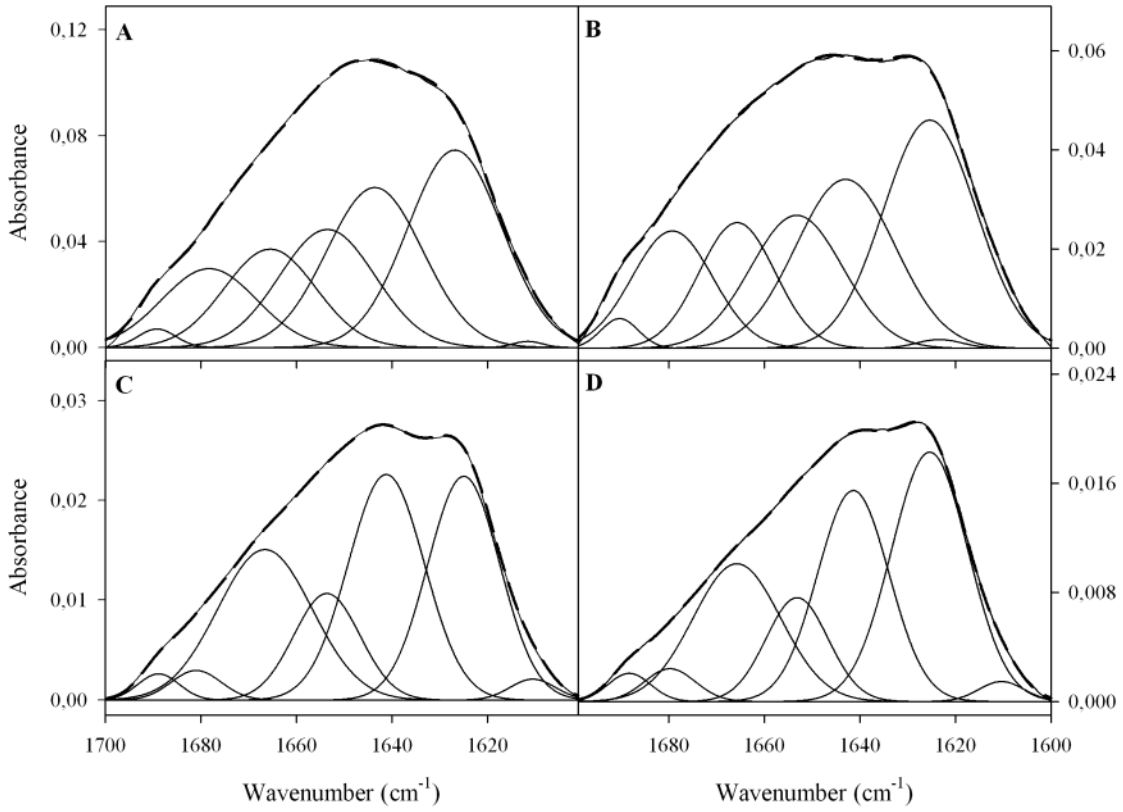

FIGURE 3: Decomposition and fitting of the FTIR spectra of the PsbO protein in H_2O (top) and in D_2O (bottom) in the presence of 1 mM $CaCl_2$ (panels A and C) or calcium depleted with 1 mM EGTA (panels B and D). The result of the fitting is shown (thick dashed line) over the real spectra (thin solid line).

The assignment of the different components of the infrared amide band to specific secondary structure elements of a protein is a key point of the results of FTIR data (*43*). The secondary structure elements usually assigned to each infrared band are indicated in Table 1. The band at 1654−1653 cm^{-1} is well reported to be assigned to α-helix plus nonordered peptide structures in H_2O, but the nonordered moves to 1643−1642 cm^{-1} in D_2O (*44*). The term nonordered assigned to the 1645−1640 cm^{-1} region corresponds to nonregular segments of the protein, i.e., mainly loops which do not represent a regular repetitive conformation, being the α-helix and β-sheet the so-called regular conformations (*43*, *44*). In general, vibrations in the 1635−1625 cm^{-1} region are assigned to β-sheet structures. β-Sheet structures also have another vibrational region at higher wavenumbers, 1690−1675 cm^{-1} (*45*). Turns, specially β-turns, partially overlap with the signal around 1679 cm^{-1}, but the turns mostly give signal together with stable loops in the 1675−1660 cm^{-1} region (*46*).

Considering these assignments, the infrared data from PsbO indicate that this protein has a major secondary structure component that corresponds to β-structure (being β-sheet, β-strand, or β-turns) and represents, in water solution in the presence of calcium, about 38% (adding the signals at 1625, 1679, and 1689 cm^{-1}) and, in heavy water in the presence of calcium, about 33% (signals at 1624, 1678, and 1688 cm^{-1}). Another very significant component corresponds to nonordered structure that accounts for about 30% (considering the 1642 cm^{-1} band in D_2O) but which can include an increase of 10−15%, if the signal from the loops (coming from the band at 1666 cm^{-1}) is added as nonregular structure. This addition makes the nonordered structure the major one in PsbO, i.e., 40−45% of total. Quantification with CD (*26*) reported a 44% random coil in PsbO, and secondary structure prediction methods indicated around 39% of loops and turns (*23*). However, the precise quantification of this type of structure is difficult because many methods only count it as "others", i.e., non-β and non-α structures.

The depletion of calcium in the solvent modifies the structural percentages, increasing the β-sheet structure from 38% to 48% in H_2O and from 33% to 39% in D_2O. The minor signal in the case of heavy water can be due to a displacement of part of the β signal to the 1666 cm^{-1} band. Due to this effect, it seems that the conformational change observed in this solvent is less apparent. However, the differences between the band at 1624 and 1666 cm^{-1} go from 4% in calcium spectra to 14% in EGTA spectra. Therefore, this suggests that the protein conformational change is not very different in H_2O and in D_2O.

The band at 1653 cm^{-1} is assigned to only α-helix in D_2O. The relative area of this band is about 11%, and it does not change too much with or without calcium. In H_2O samples, the area of the 1654 cm^{-1} band is about 21%, independent of the presence or absence of calcium. Elucidation of the amount of α-helix is not possible in H_2O alone, as the nonordered structure band overlaps with the α vibration at 1654 cm^{-1}. In D_2O this is not the case as the nonordered structure moves to the 1642 cm^{-1} band and no overlapping occurs. Therefore, the estimated amount of α-helix in PsbO is about 10%.

Figure 4A shows a series of spectra of the thermal denaturation of the PsbO protein between 20 and 80 °C in D_2O in the presence of calcium using a 3D plot. Two bands at temperatures above 70 °C appear at 1684−1686 and

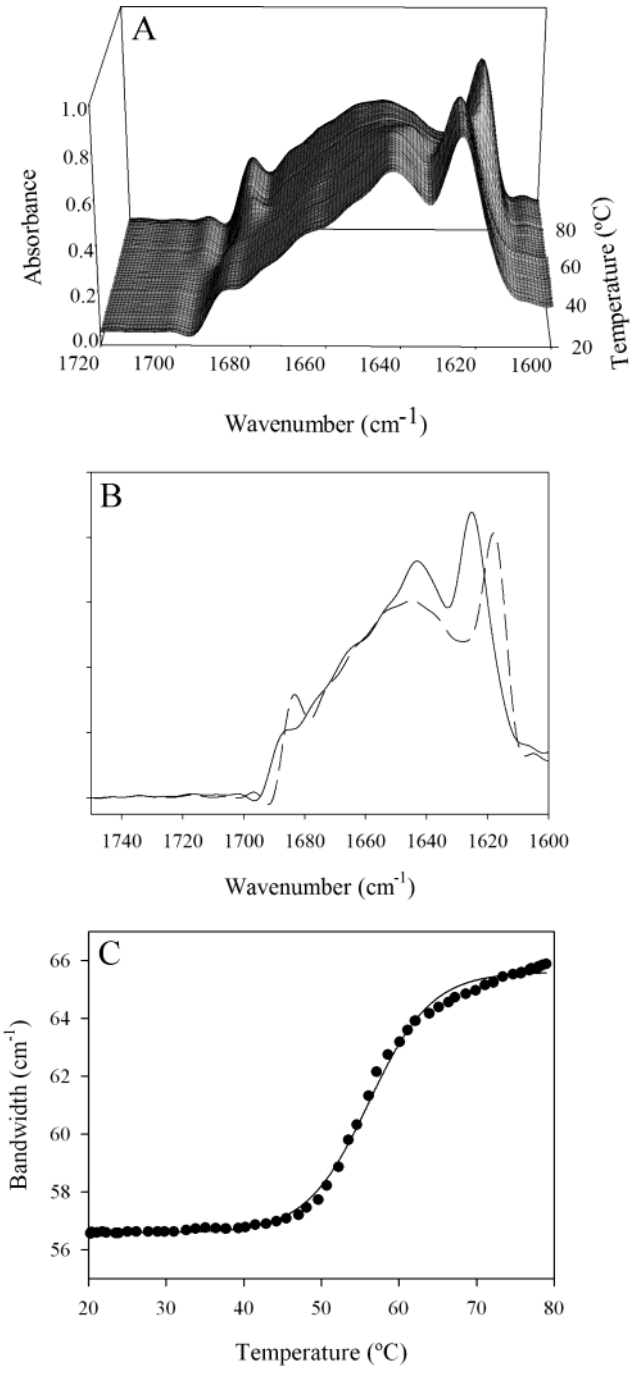

FIGURE 4: (A) 3D plot of temperature-induced denaturation between 20 and 76 °C of the PsbO protein in D_2O in the presence of 1 mM $CaCl_2$. In panel B the deconvoluted PsbO spectra at 20 °C (solid line) and 70 °C (dashed line) are plotted. In panel C a plot representing the bandwidth at half of the amplitude of the spectra of panel A versus temperature is shown.

1617−1619 cm^{-1} and can be assigned to aggregation of the protein. These two bands represent intermolecular hydrogen bonds which resemble those existing in inclusion bodies (*47*) or aggregation states (*48*). In Figure 4B, the deconvoluted spectra of the PsbO protein with $CaCl_2$ at 20 and 70 °C are shown in order to fully demonstrate that the bands at 1684−1686 and 1617−1619 cm^{-1} appear only at the end of the thermal treatment and are not present in freshly purified protein. The thermal profile is shown in Figure 4C where the bandwidth at half of the amplitude of the amide I′ band versus temperature is plotted. This figure shows a steady phase from 20 to 50 °C and a fast increase from 50 to 60 °C which includes more than 80% of the bandwidth change. This increase is related to the unfolding of PsbO and shows a melting point (T_m) value of 56 °C. After 60 °C a clear plateau is not achieved, but rather a slow increasing phase is observed in the thermal denaturation profile. We did a quantification of β-structure in the spectra at 60 °C, and we observed that a significant part of this structure is still preserved. Above 70 °C the spectral bands are clearly distorted, and the signals of aggregation appear (i.e., the mentioned bands at 1684−1686 and 1617−1619 cm^{-1}). These observations seem to indicate that the protein reaches between 60 and 70 °C an intermediate state, prior to complete denaturation, which conserves an important part of β-structure.

DISCUSSION

In this paper we show FTIR analyses where determination of PsbO secondary structures, including α-helix, β-sheet, turns, and loops (i.e., nonordered content), supports and clarifies previous quantitative results obtained by CD spectroscopy (*21*, *25*, *26*). The results suggest that in the PsbO extrinsic protein the major proportion of ordered (i.e., regular) structure corresponds to β-structure. Other reports have shown that the PsbO protein has an extended structure dominated by β-strands (*24*) probably forming a long β-barrel (*1*, *2*). It seems that at least a part of this β-structure remains unchanged even after initial temperature treatment (as commented on in Results, Figure 4). This could mean that there is a central region within the PsbO protein which needs high energy for any modification to occur and is likely to form the hydrophobic core of the protein. This agrees with results of other authors also suggesting for PsbO a mainly β-sheet conformation with a β-hydrophobic core, as shown by ANS fluorescence spectra (*26*). Another fact supporting the idea of such a hydrophobic core is the low vibrational frequency of the spectral component at the 1625−1624 cm^{-1} (β-sheet) band. This spectral component is usually assigned to hydrogen bonds typical of a compact β-sheet structure with a planar layout. However, the observation that the temperature range for when PsbO undergoes major unfolding covers just 10 °C (from 50 to 60 °C) suggests that the intramolecular interactions (hydrogen bonds, salt bridges, etc.) to keep the proper native structure of the PsbO protein may be relatively weak, and thus the unfolding of the protein occurs in a narrow range of temperature. In addition, unfolding studies of PsbO against high pressure have shown that this protein becomes unfolded at significantly lower pressures than those normally needed for unfolding other soluble proteins (*49*, *50*), which is consistent with a natively extended structure and relatively weak intramolecular interaction at least in some part of the protein. Once the protein has reached the state at 60 °C, it preserves a significant amount of β-structure, and it needs 10 °C more to show the symptoms of complete denaturation. Another temperature-induced unfolding experiment with PsbO has already been reported (*20*), and the profile is similar to the one presented here. In this way, the thermal denaturation profile seems to indicate that a part of the PsbO protein with extended β-structure can undergo a quick or energetically easy unfolding, but another part of PsbO seems to be more compact and may form a hydrophobic core more difficult

to denature. This dual nature of PsbO in solution may explain the difficulties found to clarify its main architecture and conformation (*20*, *31*, *38*).

The estimated amount of α-helix for the protein is about 10%, and this includes standard α-helices and probably some small 3_{10} helices. Data obtained by far-UV CD spectroscopy determined 9% α-helix (*25*) or 8% α-helix (*26*) for the PsbO extrinsic protein isolated from spinach. These data agree with our FTIR quantification and indicate that the α-helix is a minor structural element in the architecture of PsbO.

It has been determined by FTIR and isotope editing that the PsbO protein suffers a secondary structure change upon binding to PSII (*38*). In that paper the authors indicate that, at the point when PsbO binds to PSII, approximately 30% of the total peptide backbone undergoes a change in secondary structure, including an increase in *β*-sheet. In our work we present a novel observation of a conformational change induced by calcium in the isolated PsbO protein, which includes a 8−10% structural displacement. When the medium contains calcium, the protein seems to lie in a conformation rich in both nonordered and *β*-structure. When this cation is removed, the protein adopts a mainly *β*-structure probably due to an interconversion to *β*-sheet of a portion of the structure assigned to nonordered coil. Calcium treatment is a commonly used method to remove the PsbO protein from PSII by a mechanism related to the ability of a calcium divalent cation to disrupt the salt bridges that join the protein to the PSII. The results presented here do not discard this effect but may suggest that the interaction with PsbO is much more specific than previously thought.

Calcium (Ca^{2+}) has been identified as a cofactor essential for the proper functioning of PSII (first reported in ref *51* and reviewed in ref *33*). Several studies have shown that the removal of Ca^{2+} inhibits the oxygen evolving capability of PSII (*11*, *52*, *53*). More specific measurements of Ca^{2+} binding to PSII have shown a loss of two very high affinity Ca^{2+} binding sites upon depletion of the PsbO extrinsic protein from PSII (*35*). This study also indicated that the manganese cluster (Mn_4) interacts with two or at least one Ca^{2+} ion, and so it shows clearly that the manganese cluster needs calcium for its correct function (*35*). More recent reports indicate a direct involvement of Ca^{2+} in oxygen formation (*36*) and the binding of Ca^{2+} to one substrate water molecule of the oxygen evolving complex (*37*). Therefore, it seems that calcium is involved in the mechanism of water oxidation (*36*, *37*, *54*). In this paper we show changes in PsbO structure in the presence of calcium. So if we say that calcium "stabilizes" the correct function of the manganese cluster, and calcium seems to bind and stabilize the structure of PsbO (the manganese stabilizing protein), it seems clear that we are looking at the two faces of the same phenomenon, which is, the concerted binding of Ca^{2+} and PsbO to the manganese cluster and PSII, which is needed for the correct function of the oxygen evolving reaction. This does not mean that the calcium that binds the manganese cluster has to be the same calcium that binds PsbO, because several calcium binding sites with several different affinities have been found on studies upon PSII (*35*).

Some putative Ca^{2+} binding regions or motifs have been identified in the PSII D1 protein (*55*, *56*). If PsbO binds specifically calcium, some putative binding motifs should also be found in PsbO. Wales et al. (*57*) identified a region in the pea PsbO sequence that may form an EF hand and bind a calcium ion. This region starts in pea at E94, and it is EVSADGSVKFEE. This sequence includes the predicted vertices of a calcium coordination octahedron (*57*). In spinach PsbO, we have searched for a calcium binding motif using bioinformatic tools (*23*), and we found a motif D-...-G-x-D-...-G-G-E that starts at D97, and it is similar to PROSITE PS00330 (*58*). PS00330 is a calcium binding motif present in several types of proteins, and it is identified by the consensus pattern D-x-[LI]-x(4)-G-x-D-x-[LI]-x-G-G-x(3)-D. This motif is involved in the binding of calcium ions in a parallel *β*-roll structure. The pattern observed in spinach is not identical to the PS00330 motif, but it includes very conserved residues (the ones underlined in the pattern are conserved in all known PsbO sequences) and it is a region that partially overlaps with the region identified by Wales et al. (*57*). It is a pity that in the known structures of PSII [PDB 1FE1 (*1*) and 1IZL (*2*)] we cannot locate this putative motif within the 3D map of PsbO because the residues are not given. Calculation of the molar amount of calcium present in our experiments per mole of PsbO (protein molecular mass of 26.5 kDa and protein concentration about 30 mg/mL) indicates that using 1 mM $CaCl_2$ we have between one and two calcium ions per PsbO unit. The saturation experiments also indicate that with this amount of calcium per PsbO the observed structural change is nearly completed and more calcium does not produce further significant change. From all of these observations we can hint that probably PsbO binds calcium at a very specific ratio and through a well-defined calcium binding region.

These aspects about interaction or binding of calcium to the PsbO protein have additional physiological implications. The role of calcium in water oxidation could be ascribed not only to stabilize the manganese cluster but also to increase or decrease the affinity of the extrinsic proteins to PSII. It is well-known that calcium acts as a second messenger in a diverse range of cellular mechanisms. With the present data, it is difficult to propose a mechanism for calcium regulation of the binding of PsbO protein to the lumenal side of PSII. Considering the activation effect of calcium on oxygen evolution (*11*, *35*, *36*, *37*, *51*−*54*), we can think that PsbO calcium depletion would induce dissociation of the protein from PSII, triggering a structural change in the PsbO protein. However, from washing and reconstitution experiments (*10*, *14*, *16*, *17*) we could think that PsbO calcium depletion would induce association of the protein to PSII, since an increase in calcium levels in the lumen may provoke or stimulate the release the PsbO protein. Probably the first hypothesis is more reasonable, but it also may occur that the calcium that regulates the PsbO binding and the calcium implicated in the manganese cluster activity are different and independent. It is difficult to verify the coexistence of several independent mechanisms, though other results favor this idea: (i) some authors have said that PsbO has little or not direct role in binding the calcium ion which is required for oxygen evolution (*34*); (ii) several different calcium binding sites have been described and characterized in PSII (sites of low affinity, high affinity, and very high affinity) (*35*, *36*). Further research is needed to fully understand the overall process of binding of the PsbO extrinsic protein to the lumenal side of PSII and its function on stabilizing the manganese−calcium cluster for water

oxidation. Here we show that calcium modulates the structure of PsbO and this effect will be important for further functional studies.

REFERENCES

1. Zouni, A., Witt, H. T., Kern, J., Fromme, P., Krauss, N., Saenger, W., and Orth, P. (2001) *Nature 409*, 739−743.
2. Kamiya, N., and Shen, J.-R. (2003) *Proc. Natl. Acad. Sci. U.S.A. 100*, 98−103.
3. Hankamer, B., Morris, E., Nield, J., Carne, A., and Barber, J. (2001) *FEBS Lett. 504*, 142−151.
4. Seidler, A. (1996) *Biochim. Biophys. Acta 1277*, 35−60.
5. Shen, J. R., and Inoue, Y. (1993) *Biochemistry 32*, 1825−1832.
6. Shen, J. R., Burnap, R. L., and Inoue, Y. (1995) *Biochemistry 34*, 12661−12668.
7. Shen, J. R., Vermaas, W., and Inoue, Y. (1995) *J. Biol. Chem. 270*, 6901−6907.
8. Shen, J. R., Ikeuchi, M., and Inoue, Y. (1997) *J. Biol. Chem. 272*, 17821−17826.
9. Bricker, T. M. (1992) *Biochemistry 31*, 4623−4628.
10. Enami, I., Yoshihara, S., Tohri, A., Okumura, A., Ohta, H., and Shen, J. R. (2000) *Plant Cell Physiol. 41*, 1354−1364.
11. Miyao, M., and Murata, N. (1984) *FEBS Lett. 170*, 350−354.
12. Mei, R., Green, J. P., Sayre, R. T., and Frasch, W. D. (1989) *Biochemistry 28*, 5560−5567.
13. Åkerlund, H. E., and Jansson, C. (1981) *FEBS Lett. 124*, 229−232.
14. Ono, T., and Inoue, Y. (1983) *FEBS Lett. 164*, 252−260.
15. Miyao, M., and Murata, N. (1983) *FEBS Lett. 164*, 375−378.
16. Yamamoto, Y., Ishikawa, Y., Nakatani, E., Yamada, M., Zhang, H., and Wydrzynski, T. (1998) *Biochemistry 37*, 1565−1574.
17. Enami, I., Kamo, M., Ohta, H., Takahashi, S., Miura, T., Kusayanagi, M., Tanabe, S., Kamei, A., Motoki, A., and Hirano, M. (1998) *J. Biol. Chem. 273*, 4629−4634.
18. Motoki, A., Shimazu, T., Hirano, M., and Katoh, S. (1998) *Biochim. Biophys. Acta 1365*, 492−502.
19. Frankel, L. K., Cruz, J. A., and Bricker, T. M. (1999) *Biochemistry 38*, 14271−14278.
20. Lydakis-Simantiris, N., Hutchison, R. S., Betts, S. D., Barry, B. A., and Yocum, C. F. (1999) *Biochemistry 38*, 404−414.
21. Motoki, A., Usui, M., Shimazu, T., Hirano, M., and Katoh, S. (2002) *J. Biol. Chem. 277*, 14747−14756.
22. Bricker, T. M., and Frankel, L. K. (1998) *Photosynth. Res. 56*, 157−173.
23. De Las Rivas, J., and Heredia, P. (1999) *Photosynth. Res. 61*, 11−21.
24. Pazos, F., Heredia, P., Valencia, A., and De Las Rivas, J. (2001) *Proteins 45*, 372−381.
25. Xu, Q., Nelson, J., and Bricker, T. M. (1994) *Biochim. Biophys. Acta 1188*, 427−431.
26. Shutova, T., Irrgang, K. D., Shubin, V., Klimov, V. V., and Renger, G. (1997) *Biochemistry 36*, 6350−6358.
27. Sonoyama, M., Motoki, A., Okamoto, G., Hirano, M., Ishida, H., and Katoh, S. (1996) *Biochim. Biophys. Acta 1297*, 167−170.
28. Ahmed, A., Tajmir-Riahi, H. A., and Carpentier, R. (1995) *FEBS Lett. 363*, 65−68.
29. Shutova, T., Deikus, G., Irrgang, K. D., Klimov, V. V., and Renger, G. (2001) *Biochim. Biophys. Acta 1504*, 371−378.
30. Zubrzycki, I. Z., Frankel, L. K., Russo, P. S., and Bricker, T. M. (1998) *Biochemistry 37*, 13553−13558.
31. Shutova, T., Irrgang, K., Klimov, V. V., and Renger, G. (2000) *FEBS Lett. 467*, 137−140.
32. Anati, R., and Adir, N. (2000) *Photosynth. Res. 64*, 167−177.
33. Debus, R. J. (1992) *Biochim. Biophys. Acta 1102*, 269−352.
34. Seidler, A., and Rutherford, A. W. (1996) *Biochemistry 35*, 12104−12110.
35. Grove, G. N., and Brudvig, G. W. (1998) *Biochemistry 37*, 1532−1539.
36. Vrettos, J. S., Stone, D. A., and Brudvig, G. W. (2001) *Biochemistry 40*, 7937−7945.
37. Hendry, G., and Wydrzynski, T. (2003) *Biochemistry 42*, 6209−6217.
38. Hutchison, R. S., Betts, S. D., Yocum, C. F., and Barry, B. A. (1998) *Biochemistry 37*, 5643−5653.
39. Berthold, D. A., Babcock, G. T., and Yocum, C. F. (1981) *FEBS Lett. 61*, 231−234.
40. Arellano, J. B., Schröder, W. P., Sandman, G., Chueca, A., and Barón, M. (1994) *Physiol. Plant. 91*, 369−374.
41. Laemmli, U. K. (1970) *Nature 227*, 680−685.
42. De Las Rivas, J., and Barber, J. (1997) *Biochemistry 36*, 8897−8903.
43. Arrondo, J. L. R., Muga, A., Castresana, J., and Goñi, F. M. (1993) *Prog. Biophys. Mol. Biol. 59*, 23−56.
44. Haris, P. I., and Chapman, D. (1995) *Biopolymers 37*, 251−263.
45. Barth, A. (2000) *Prog. Biophys. Mol. Biol. 74*, 141−173.
46. Goormaghtigh, E., Cabiaux, V., and Ruysschaert, J. M. (1990) *Eur. J. Biochem. 193*, 409−420.
47. Dong, A. C., Prestreslki, S. J., Allison, S. D., and Carpenter, J. F. (1995) *J. Pharm. Sci. 84*, 415−424.
48. Fink, A. L., Seshandri, S., Khurana, R., and Oberg, K. A. (1999) in *Infrared analysis of peptides and proteins* (Singh, B. R., Ed.) American Chemical Society, Washington, DC.
49. Ruan, K., Xu, C., Yu, Y., Li, J., Lange, R., Bec, N., and Balny, C. (2001) *Eur. J. Biochem. 268*, 2742−2750.
50. Ruan, K., Xu, C., Li, T., Li, J., Lange, R., and Balny, C. (2003) *Eur. J. Biochem. 270*, 1654−1661.
51. Brand, J. J., and Becker, D. W. (1984) *J. Bioenerg. Biomembr. 16*, 239−249.
52. Ghanotakis, D. F., Topper, J. N., Babcock, G. T., and Yocum, C. F. (1984) *FEBS Lett. 167*, 127−130.
53. Nakatani, H. Y. (1984) *Biochem. Biophys. Res. Commun. 121*, 626−633.
54. Rajendiran, M., Caudle, T., Kirk, M. L., Setyawati, I., Kampf, J. W., and Pecoraro, V. L. (2003) *J. Biol. Inorg. Chem. 8*, 283−293.
55. Qian, M., Dao, L., Debus, R. J., and Burnap, R. (1999) *Biochemistry 38*, 6070−6081.
56. Li, Z. L., and Burnap, R. L. (2001) *Biochemistry 40*, 10350−10359.
57. Wales, R., Newman, B. J., Pappin, D., and Gray, J. C. (1989) *Plant Mol. Biol., Int. J. Mol. Biol., Biochem., Genet., Eng. 12*, 439−451.
58. Baumann, U., Wu, S., Flaherty, K. M., and McKay, D. B. (1993) *EMBO J. 12*, 3357−3364.

BI034582J